Solar Cells, 5 (1982) 143 - 172

EFFECT OF THE BACK-SURFACE FIELD ON THE OPEN-CIRCUIT VOLTAGES OF p^+–n–n^+ AND n^+–p–p^+ SILICON SOLAR CELLS

S. N. SINGH and G. C. JAIN

Division of Materials, National Physical Laboratory, New Delhi 110012 (India)

(Received February 10, 1981; accepted June 9, 1981)

Summary

The effect of the back-surface field (BSF) on the open-circuit voltages V_{oc} of front-illuminated p^+–n–n^+ (p/n BSF) and n^+–p–p^+ (n/p BSF) silicon solar cells was investigated. A theory based on the assumption that the front emitter has a unit injection efficiency was formulated and this theory can be applied to both low and high level conditions in the bulk regions of p/n and n/p BSF cells. The effect of perfect and imperfect minority carrier blocking at the low–high (L–H) junction end of the bulk region was analysed. The theory gives some insight into the physics of the BSF cells. It shows that the minority carrier blocking at the L–H back junction both by itself and by causing a back reflection of minority carriers towards the front-junction end of the bulk region leads to an improvement in the open-circuit voltage of the cells. The contribution of back reflection is independent of the intensity of illumination and the resistivity ρ_B of the bulk region, whereas the contribution of minority carrier blocking increases with both the intensity of illumination and ρ_B. For low level conditions the improvement in V_{oc} is mainly due to the contribution of back reflection. However, for high level conditions the contribution of minority carrier blocking can be quite large. For high level conditions the increase in recombination at the front surface and in the front region is more harmful to the V_{oc} value of a p/n BSF cell. However, a decrease in the minority carrier blocking at the L–H junction is more harmful to the V_{oc} value of an n/p BSF cell. The fact that V_{oc} for BSF cells is independent of ρ_B is attributed to the high level conditions in their bulk regions.

1. Introduction

It has been established that a back-surface field (BSF) can lead to a substantial increase in the short-circuit current density J_{sc}, the open-circuit voltage V_{oc} and the curve factor of an n^+–p–p^+ (or p^+–n–n^+) silicon solar cell [1 - 4]. Many workers [1 - 3, 5 - 13] have attempted to explain the phenomenon governing the functioning of BSF cells. Godlewski *et al.* [8] showed that if $d/L > 3$, where d is the distance between the p–n front and low–high (L–H)

0379-6787/82/0000-0000/$02.75

junctions and L is the diffusion length of minority carriers in the bulk region, the L–H back junction cannot significantly influence the performance of a silicon solar cell. Mandelkorn and Lamneck [2] concluded that the improvement in V_{oc} for an n^+–p–p^+ cell is due to the additional photovoltage developed at the L–H back junction. Mandelkorn and Lamneck's [2] findings set an upper limit for ΔV_{oc} such that ΔV_{oc} cannot be more than kT/q unless the bulk region of the cell acquires high level conditions in it. For front-illuminated n^+–p–p^+ silicon cells with $\rho_B = 10\ \Omega$ cm and $V_{oc} < 0.588$ V at 300 K, as high level conditions in their bulk regions cannot be fulfilled, the observed ΔV_{oc} of about 50 mV [1] cannot be due to the above reason. Fossum [11] gave an analytical description of the performance of the n^+–p–p^+ cell. Owing to the assumption of a very large lifetime of minority carriers in the bulk region, however, the validity of the above analytical description [11] is limited to cells with $d/L \ll 1$. Recently, von Roos [12, 13] has analysed the BSF effect in an n^+–p–p^+ cell by considering the front and back junctions as two capacitors connected in series and has shown that such a model can explain the increase in J_{sc} and V_{oc} due to the BSF. There are relatively fewer studies on p^+–n–n^+ BSF cells [2, 3]. Fossum and Burgess [3] found that the front-surface recombination had a very significant influence on the open-circuit voltage of their high efficiency p^+–n–n^+ cells.

Although BSF cells have been discussed extensively in recent literature [1 - 16], a comprehensive theory of the BSF effect is still lacking. In this paper we present an analytical approach which is an attempt to investigate how the BSF improves V_{oc} for silicon solar cells.

This analysis is based on the concept of effective recombination velocity of minority carriers at the back of the bulk region and a unit injection efficiency of the p^+ (n^+) front emitter of p^+–n–n^+ (n^+–p–p^+) solar cells. A general theory for the BSF will be formulated and will subsequently be used to discuss the effect of the BSF on J_{sc} and V_{oc}. The effect of the BSF on V_{oc} will be analysed in detail for both low and high level conditions in the bulk region. Conditions where the analysis is not applicable will also be discussed.

Before proceeding to formulate the general theory of the BSF it is appropriate to discuss first a few important parameters and phenomena relevant to the analysis.

2. Minority carrier blocking, back reflection and back-contact recombination velocity

An ohmic contact on the back of the bulk n (or p) region of a p^+–n (or an n^+–p) solar cell which has a theoretically infinite and a practically very high recombination velocity for minority carriers [17] means that the minority carrier density at the end of the bulk region near this contact is fixed at its equilibrium value under all stages of operation between short-circuit and open-circuit conditions. In contrast, the ohmic contact on the back of a p^+–n–n^+ (n^+–p–p^+) solar cell has no direct control over the density of minority carriers at the back end of the bulk region. This is because there is an L–H potential barrier and an n^+ (p^+) layer between them. The built-in field at the L–H potential barrier, *i.e.* the n–n^+ (p–p^+) junction, favours passage of the majority electrons (holes) and opposes the passage of the minority holes (electrons) from the bulk n (p) region to the n^+ (p^+) region on the back. This blocking of minority carriers results in the back reflection of minority carriers to the front-junction end of the bulk region and their piling-up at the L–H junction end of the bulk region. The blocking ability of the L–H back junction will depend on (i) the barrier height of the L–H back junction, (ii) the recombination in the space charge region at the L–H junction and (iii) the magnitude of the minority carrier current in the n^+ (p^+) region at the edge of the L–H junction. However, its effectiveness will also depend on d/L.

Back reflection depends on d/L and the minority-carrier-blocking ability of the L–H back junction. The effect of the BSF on the performance of a solar cell can be evaluated by defining an effective recombination velocity S of minority carriers at the L–H junction end of its bulk region. S represents a collective effect of the three factors (i) - (iii). $S = \infty$ would mean the worst L–H junction contact, virtually equivalent to an ohmic contact at the bulk region itself. $S = 0$, however, would normally mean perfect blocking or majority carrier contact onto the back of the bulk n region. In the following, p^+–n–n^+ cells will be dealt with, with occasional reference to n^+–p–p^+ cells.

For a p^+–n–n^+ cell, S is a minimum if the total current density at the rear end of the bulk n region is almost entirely due to electrons. This is possible if the recombination current in the space charge layer is negligible and the minority hole current in the n^+ region at the edge of the space charge layer at the n–n^+ junction is also negligible. In practice, it may be achieved by forming a thick and heavily doped n^+ region on good quality and damage-free n-type silicon and minimizing the creation of defects during its formation. It should be obvious that S is likely to be lower for a p^+–n–n^+ silicon solar cell made using a high purity single-crystal wafer than for one made using a less pure or polycrystalline silicon wafer. In further discussion, only single-crystal cells will be considered.

3. Low and high level conditions in the bulk region

At any stage of operation of a p^+–n or p^+–n–n^+ solar cell between short-circuit and open-circuit conditions, let p be the density of holes at any point X in the n-type region and N_D be the base doping in it. The portion of the n-type region where $p < N_D$ will operate under low level conditions. However, the portion where $p > N_D$ will have high level conditions in it. Depending on N_D and the intensity of illumination, we can always manage to have low level conditions throughout the n region of a p^+–n or a p^+–n–n^+ cell. However, even at a very high intensity of illumination a p^+–n or a p^+–n–n^+ silicon solar cell may not have a high level condition throughout its n region at or close to the short circuit when the diode current is either zero or negligible compared with the short-circuit current.

An increase in the diode current that flows against the photocurrent raises the minority carrier density in the bulk region at the edge of the space charge layer at the p–n junction of a p^+–n, p^+–n–n^+, n^+–p or n^+–p–p^+ cell above the thermal equilibrium values. For p^+–n–n^+ and n^+–p–p^+ cells there is an increase in the minority carrier density at the rear end of the bulk region also. The diode current reaches its maximum in the open-circuit condition and so does the minority carrier density in the bulk region at the edge of the p–n junction. Thus, should high level conditions prevail in the bulk region, either all or the maximum amount of the bulk region of a p^+–n or p^+–n–n^+ silicon solar cell will experience high level conditions for an open circuit. The hole density p_0 at the p^+–n junction end of the bulk n region is also then a maximum, being equal to $p_{0\,max}$. For small current densities the diode current in the bulk n region at the edge of the p–n junction is mostly due to holes [18, 19]. This should also be valid for properly designed silicon solar cells for which recombination in the front p^+ region as well as at the exposed surface at the top is negligible compared with that in the bulk region. Under such conditions, $p_{0\,max}$ is also normally the maximum hole density at any point (in a one-dimensional model) in the bulk region.

Let the reduction in the barrier height at the p–n junction be denoted by V_J. Now, defining

$$V_{J0} = \frac{2kT}{q} \ln\left(\frac{N_D}{n_i}\right)$$

and comparing V_{oc} with V_{J0}, the low and high level conditions in the bulk region of an illuminated p/n cell at open circuit can easily be obtained. If $V_{oc} < V_{J0}$, there will be low level conditions throughout the bulk region. However, if $V_{oc} > V_{J0}$, the high level conditions will occur either in the entire bulk n region or in a part of it on the p–n junction side. This is so because V_{oc} is entirely due to V_J unless high level conditions prevail in the bulk region. Strictly, for a BSF cell with low level conditions in the bulk region, $V_{oc} - V_J < kT/q$. The conditions $V_{oc} < V_{J0}$ and $V_{oc} > V_{J0}$ correspond to $p_{0\,max}/N_D < 1$ and $p_{0\,max}/N_D > 1$ respectively. V_{J0} can be related to ρ_B by

$$V_{J0} = \frac{2kT}{q} \ln(\rho_B n_i q \mu_n)^{-1} \qquad (1)$$

Similarly, for an n/p cell, V_{J0} and ρ_B can be related by

$$V_{J0} = \frac{2kT}{q} \ln(\rho_B n_i q \mu_p)^{-1} \qquad (2)$$

In eqns. (1) and (2), n_i is the intrinsic carrier density at T and μ_n and μ_p are the electron mobility and hole mobility respectively. V_{J0} as a function of ρ_B, as given by eqns. (1) and (2), is plotted in Fig. 1 for p/n and n/p silicon cells (BSF or conventional) at T = 300 K. The dependences of μ_n and μ_p on ρ_B (or on ionized impurity concentration) have been taken into account [20]

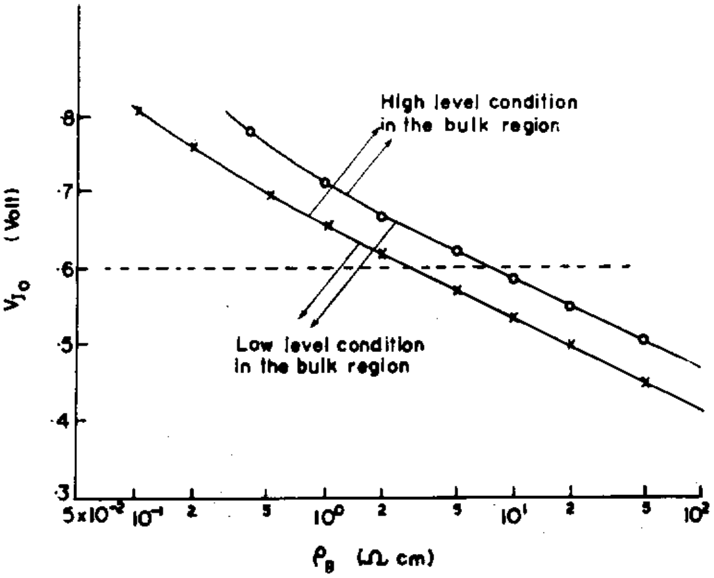

Fig. 1. V_{J0} (the minimum barrier height reduction at the p–n junction required for high level conditions to prevail in the bulk region of a cell) as a function of the bulk resistivity ρ_B of silicon p/n or n/p BSF (of conventional) solar cells at T = 27 °C (300 K): ○, p-type bulk region; ×, n-type bulk region. A cell will have high level conditions in its bulk region if its V_{oc} is greater than V_{J0}.

in plotting these curves. It is important to note that, for equal ρ_B values, a p/n cell has a lower V_{J0} than has an n/p cell. This implies that a p/n cell can have high level conditions at a lower V_{oc} than an n/p cell of equal ρ_B can. For $V_{oc} \geqslant 0.6$ V at 300 K, however, both p/n and n/p silicon cells will have high level conditions in their bulk regions provided that $\rho_B > 4$ Ω cm for p/n cells and $\rho_B > 10$ Ω cm for n/p cells. A situation may arise in practice in which a cell without a BSF operates under low level conditions and with the addition of a BSF attains high level conditions in its bulk region. A comprehensive theory of BSF solar cells should be applicable even to such cases where low and high level conditions may not be well defined.

4. General theory of back-surface field cells

Figure 2 shows a front-illuminated p^+–n–n^+ cell schematically. The front surface is shown to be at $x = -d_p$ and the L–H junction at $x = d$. A one-dimensional theory of BSF cells can be formulated. The following assumptions are made.

(i) The entire front surface of the cell is uniformly illuminated, and carrier transport and photon travel are restricted along the x direction.

(ii) The bulk n region is uniformly doped and quasi-neutrality conditions are valid.

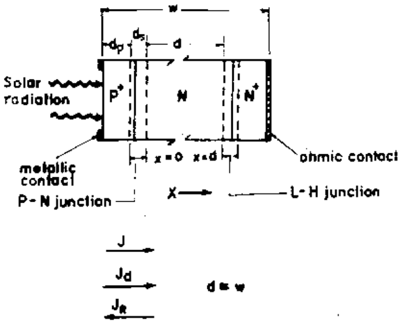

Fig. 2. A schematic diagram of a front-illuminated p^+–n–n^+ solar cell: $x = 0$, the front end of the bulk region on the p–n front-junction side; $x = d$, the rear end of the bulk region on the L–H back-junction side; p–n, p^+–n junction of a p^+–n–n^+ cell; L–H, n–n^+ junction of a p^+–n–n^+ cell.

(iii) The cell is maintained at room temperature T.

(iv) Shockley–Read–Hall recombination statistics [21] are applicable.

(v) Carrier mobilities and the lifetime of excess carriers are spatially invariant in the n region.

The total current density J can be computed by adding the hole and electron current densities. Therefore

$$J = J_p|_{x=0} + J_n|_{x=0} \tag{3a}$$

where $J_p|_{x=0}$ and $J_n|_{x=0}$ are the hole current density and the electron current density respectively at $x = 0$ (Fig. 2). Also

$$J = J_n|_{x=-d_s} + J_p|_{x=0} + J_{sp} \tag{3b}$$

where $J_n|_{x=-d_s}$ is the electron current density in the p^+ front region at $x = -d_s$ (Fig. 2) and J_{sp} is the space charge recombination current density in the depletion layer at the p^+–n junction. Equation (3a) shows that

$$J \approx J_p|_{x=0} \tag{4}$$

if

$$J_n|_{x=0} \ll J_p|_{x=0} \tag{5}$$

Equation (3b) shows that inequality (5) and hence eqn. (4) can be valid if $J_n|_{x=-d_s}$ and J_{sp} are much less than $J_p|_{x=0}$. The validity of eqn. (4) implies that for dark conditions the p^+ emitter has a unit injection efficiency. Under illuminated conditions, J can be expressed as

$$J = J_d - J_R \tag{6}$$

where J_d is the diode (or dark) current density of the solar cell and J_R is the photocurrent density of the solar cell.

Thus, for illuminated conditions the identification of $J = J_p|_{x=0}$ with eqn. (6) would imply the twin assumptions (a) that J_d is due to the injection of holes into the bulk n region at $x = 0$, *i.e.* the p^+ front emitter has a unit injection efficiency [18, 19], and (b) that J_R is due to the collection of holes from the bulk n region.

The assumption (a) can be valid if the minority carrier recombination at the front surface, in the p^+ front region and in the space charge region at the front junction have negligible contributions to the total diode current density compared with the contribution of recombination in the bulk region and at the back surface [18, 19]. The assumption (b) can be valid if contributions of the photogenerated carriers collected from the front and the space charge regions to the total photocurrent are negligible compared with that of holes collected from the bulk region.

In practice the unit injection efficiency of the front emitter can be achieved by minimizing the adverse effects of heavy doping in the front region (*e.g.* the creation of a dead layer [22] and band gap narrowing [23]), creating a built-in electric field due to impurity gradient in the front region [24] and reducing the front-surface recombination, *e.g.* by covering the front exposed surface with a thin layer of SiO_2 before coating it with an antireflection film [3]. However, practically J_R can be due to the contribution of holes from the bulk n region if the front p^+ region is shallow and both the cell thickness w ($\approx d$) and the diffusion length of holes in the bulk n region are large.

It may be mentioned that inequality (5) cannot hold for $J = 0$. However, it can hold for $J \to 0$. Therefore, strictly, eqn. (4) would not be valid for $J = 0$. However, it can hold for $J \to 0$ and can be applicable to the open-circuit condition in practice.

From the basic theory of carrier transport in a semiconductor it is known that

$$J_p = pq\mu_p E - qD_p \frac{dp}{dx}$$

and

$$J_n = nq\mu_n E + qD_n \frac{dn}{dx}$$

where E is the electric field in the bulk n region. Further, quasi-neutrality conditions in the n region give

$$N_D + p \approx n$$

$$\frac{dp}{dx} \approx \frac{dn}{dx}$$

Using quasi-neutrality conditions, the total current density $J = J_p + J_n$ is given by

$$J = \{p(\mu_p + \mu_n) + N_D\mu_n\}qE + q(D_n - D_p)\frac{dp}{dx}$$

Incorporating Einstein's relationships for non-degenerate conditions

$$\frac{D_p}{\mu_p} = \frac{D_n}{\mu_n} = \frac{kT}{q}$$

and defining $b = \mu_n/\mu_p$ we have

$$J_p = \frac{pJ}{p(b+1)+bN_D} - qD_n \frac{2p+N_D}{p(b+1)+bN_D}\frac{dp}{dx} \qquad (7)$$

and hence

$$J_p|_{x=0} = \frac{p_0 J}{p_0(b+1)+bN_D} - qD_n \frac{2p_0+N_D}{p_0(b+1)+bN_D}\left.\frac{dp}{dx}\right|_{x=0} \qquad (8)$$

Since $J \approx J_p|_{x=0}$, hence

$$J \approx -qD_p \frac{2p_0+N_D}{p_0+N_D}\left.\frac{dp}{dx}\right|_{x=0} \qquad (9)$$

where p_0 and $(dp/dx)|_{x=0}$ are the values of p and dp/dx at $x = 0$ in the bulk n region. Computation of J requires determination of the values of p_0 and $(dp/dx)|_{x=0}$.

4.1. Computation of J

Under steady state conditions the continuity equation for holes in the n region of a front-illuminated p$^+$–n–n$^+$ solar cell is [25]

$$\frac{d^2p}{dx^2} = \frac{p-p_n}{L^2} - \sum_{\lambda=\lambda_{min}}^{\lambda=\lambda_g} \frac{n_{ph}(1-R_\lambda)}{D_p L_\lambda}\exp\left(-\frac{d_p+d_s+x}{L_\lambda}\right) \qquad (10)$$

where λ_{min} is the minimum value of λ for a multiwavelength source below which the radiation would make a negligible contribution to the photon current density in the cell. For the solar spectrum, $\lambda_{min} = 0.28\ \mu m$. λ_g is the cut-off wavelength ($\lambda_g = hc/E_g$) and depends on the forbidden energy gap of the semiconductor material of the junction. n_{ph}, R_λ and L_λ are functions of λ and the second term on the right-hand side of eqn. (10) is a summation for radiations of various wavelengths between λ_{min} and λ_g.

A general solution of eqn. (10) is given by

$$p = p_n + A\exp\left(-\frac{x}{L}\right) + B\exp\left(\frac{x}{L}\right) - \sum \frac{n_{ph}(1-R_\lambda)L^2 L_\lambda}{D_p(L^2-L_\lambda^2)}\exp\left(-\frac{d_p+d_s+x}{L_\lambda}\right) \qquad (11)$$

The constants A and B in eqn. (11) can be evaluated using the boundary conditions

$$p = p_0 = p_n \exp\left(\frac{qV_J}{kT}\right) \qquad \text{at } x = 0 \qquad (12)$$

$$p = p_d \qquad \text{at } x = d \qquad (13)$$

The values of the constants A and B are given by

$$A = \frac{[p_0 - p_n + \Sigma N_0 \exp\{-(d_p + d_s)/L_\lambda\}] \exp(d/L) - \{p_d - p_n + \Sigma N_0 \exp(-w/L_\lambda)\}}{2 \sinh(d/L)} \tag{14}$$

and

$$B = \frac{\{p_d - p_n + \Sigma N_0 \exp(-w/L_\lambda)\} - [p_0 - p_n + \Sigma N_0 \exp\{-(d_p + d_s)/L_\lambda\}] \exp(-d/L)}{2 \sinh(d/L)} \tag{15}$$

respectively. In eqns. (14) and (15)

$$N_0 = \frac{(1 - R_\lambda) n_{ph} L^2 L_\lambda}{D_p (L^2 - L_\lambda{}^2)} \tag{16}$$

and

$$w = d_p + d_s + x$$

From eqn. (11),

$$\left.\frac{dp}{dx}\right|_{x=0} = \frac{B - A}{L} + \sum \frac{N_0}{L_\lambda} \exp\left(-\frac{d_p + d_s}{L_\lambda}\right) \tag{17}$$

Equations (14), (15) and (17) can be used to yield the total current density J in eqn. (9):

$$J = qD_p \frac{2p_0 + N_D}{p_0 + N_D} \left\{ p_0 - p_n + \sum N_0 \exp\left(-\frac{d_p + d_s}{L_\lambda}\right)\right\} \frac{\coth(d/L)}{L} - - qD_p \frac{2p_0 + N_D}{p_0 + N_D} \left\{ \sum \frac{N_0}{L_\lambda} \exp\left(-\frac{d_p + d_s}{L_\lambda}\right) + + \frac{\operatorname{cosech}(d/L)}{L} \sum N_0 \exp\left(-\frac{w}{L_\lambda}\right)\right\} - qD_p \frac{2p_0 + N_D}{p_0 + N_D} \frac{p_d - p_n}{L \sinh(d/L)} \tag{18}$$

To compute J from eqn. (18) it is necessary to determine $p_d - p_n$.

The hole current density at $x = d$ can be described by

$$J_p|_{x=d} = qS(p_d - p_n) \tag{19}$$

where S is the effective recombination velocity of holes at $x = d$, as defined in Section 2. Also, $J_p|_{x=d}$ is given from eqn. (7) as

$$J_p|_{x=d} = \frac{p_d J}{p_d(b+1) + bN_D} - qD_n \frac{2p_d + N_D}{p_d(b+1) + bN_D} \left.\frac{dp}{dx}\right|_{x=d} \tag{20}$$

and $(dp/dx)|_{x=d}$ is given from eqn. (11) as

$$\left.\frac{dp}{dx}\right|_{x=d} = \frac{1}{L}\left\{B \exp\left(\frac{d}{L}\right) - A \exp\left(-\frac{d}{L}\right)\right\} + \sum \frac{N_0}{L_\lambda} \exp\left(-\frac{w}{L_\lambda}\right)$$

or

$$\left.\frac{\mathrm{d}p}{\mathrm{d}x}\right|_{x=d} = \left\{p_d - p_\mathrm{n} + \sum N_0 \exp\left(-\frac{w}{L_\lambda}\right)\right\} \frac{\coth(d/L)}{L} - \\ - \frac{1}{L \sinh(d/L)} \left\{p_0 - p_\mathrm{n} + \sum N_0 \exp\left(-\frac{d_\mathrm{p} + d_\mathrm{s}}{L_\lambda}\right)\right\} + \\ + \sum \frac{N_0}{L_\lambda} \exp\left(-\frac{w}{L_\lambda}\right) \tag{21}$$

Substituting eqn. (21) into eqn. (20) and then equating the resultant with eqn. (19), we can obtain

$$p_d - p_\mathrm{n} = \frac{p_d J(L/D^*) \tanh(d/L)}{q\{p_d(b+1) + bN_\mathrm{D}\}\{1 + \epsilon \tanh(d/L)\}} + \\ + \left(\frac{[p_0 - p_\mathrm{n} + \Sigma N_0 \exp\{-(d_\mathrm{p} + d_\mathrm{s})/L_\lambda\}] \operatorname{sech}(d/L)}{1 + \epsilon \tanh(d/L)} - \\ - \frac{\Sigma N_0 \exp(-w/L_\lambda) + L \tanh(d/L) \Sigma (N_0/L_\lambda) \exp(-w/L_\lambda)}{1 + \epsilon \tanh(d/L)}\right) \tag{22}$$

where

$$\epsilon = SL/D^* \tag{23}$$

and

$$D^* = \frac{D_\mathrm{n}(2p_d + N_\mathrm{D})}{p_d(b+1) + bN_\mathrm{D}} \tag{24}$$

D^* can be approximated to D_p and $2D_\mathrm{p}D_\mathrm{n}/(D_\mathrm{p} + D_\mathrm{n})$ for low and high level conditions respectively. For high level conditions, L will represent the ambipolar diffusion length of carriers in the bulk region. From eqns. (19), (20) and (23) it can be noted that $\epsilon = 0$ (*i.e.* $S = 0$) corresponds to $(\mathrm{d}p/\mathrm{d}x)|_{x=d} = 0$ and $(\mathrm{d}p/\mathrm{d}x)|_{x=d} < 0$ for $\epsilon > 0$.

In eqn. (22) the first term on the right-hand side is zero under open-circuit conditions ($J \to 0$). It is negligible compared with the second term under short-circuit conditions also. Therefore

$$p_d - p_\mathrm{n} = \frac{[p_0 - p_\mathrm{n} + \Sigma N_0 \exp\{-(d_\mathrm{p} + d_\mathrm{s})/L_\lambda\}] \operatorname{sech}(d/L)}{1 + \epsilon \tanh(d/L)} - \\ - \frac{\Sigma N_0 \exp(-w/L_\lambda) - L \tanh(d/L) \Sigma (N_0/L_\lambda) \exp(-w/L_\lambda)}{1 + \epsilon \tanh(d/L)} \tag{25}$$

would be valid for both short-circuit and open-circuit conditions. Substituting the value of $p_d - p_\mathrm{n}$ from eqn. (25) into eqn. (18) gives

$$J = qD_p \frac{2p_0 + N_D}{p_0 + N_D} \frac{p_0 - p_n}{L} \frac{\epsilon + \tanh(d/L)}{1 + \epsilon \tanh(d/L)} +$$

$$+ qD_p \frac{2p_0 + N_D}{p_0 + N_D} \left\{ \frac{\epsilon + \tanh(d/L)}{L\{1 + \epsilon \tanh(d/L)\}} \sum N_0 \exp\left(-\frac{d_p + d_s}{L_\lambda}\right) + \right.$$

$$\left. + \frac{\operatorname{sech}(d/L)}{1 + \epsilon \tanh(d/L)} \sum N_0 \exp\left(-\frac{w}{L_\lambda}\right) \right\} -$$

$$- qD_p \frac{2p_0 + N_D}{p_0 + N_D} \left[\sum \frac{N_0}{L_\lambda} \exp\left(-\frac{d_p + d_s}{L_\lambda}\right) + \right.$$

$$\left. + \frac{\epsilon \operatorname{sech}(d/L)}{L\{1 + \epsilon \tanh(d/L)\}} \sum N_0 \exp\left(-\frac{w}{L_\lambda}\right) \right] \tag{26}$$

The first term on the right-hand side of eqn. (26) gives essentially the contribution of the bulk region to the total dark current density or the diode current density when not illuminated. It can be equated to J_d if the contributions of the front region and the space charge region at the front junction to J_d are negligible. The second and third terms depend on N_0 and give the contribution of the bulk region to the total photocurrent density. This contribution can be equated to J_R if the contributions of the front region and the space charge region at the front junction to J_R are negligible.

Therefore, because the twin assumptions (a) and (b) discussed earlier are valid, we can write

$$J_d = qD_p \frac{2p_0 + N_D}{p_0 + N_D} \frac{p_0 - p_n}{L} \frac{\epsilon + \tanh(d/L)}{1 + \epsilon \tanh(d/L)} \tag{27}$$

and

$$J_R = qD_p \frac{2p_0 + N_D}{p_0 + N_D} \left[\sum \frac{N_0}{L_\lambda} \exp\left(-\frac{d_p + d_s}{L_\lambda}\right) + \right.$$

$$\left. + \frac{\epsilon \operatorname{sech}(d/L)}{L\{1 + \epsilon \tanh(d/L)\}} \sum N_0 \exp\left(-\frac{w}{L_\lambda}\right) \right] -$$

$$- qD_p \frac{2p_0 + N_D}{p_0 + N_D} \left[\frac{\epsilon + \tanh(d/L)}{L\{1 + \epsilon \tanh(d/L)\}} \sum N_0 \exp\left(-\frac{d_p + d_s}{L_\lambda}\right) + \right.$$

$$\left. + \frac{\operatorname{sech}(d/L)}{1 + \epsilon \tanh(d/L)} \sum \frac{N_0}{L_\lambda} \exp\left(-\frac{w}{L_\lambda}\right) \right] \tag{28}$$

Equations (27) and (28) hold if (a) assumptions (i) - (v) and eqn. (4) are valid and (b) the condition

$$\left.\frac{\mathrm{d}p}{\mathrm{d}x}\right|_{x=d} \leqslant 0 \tag{29}$$

is satisfied.

Condition (29) originates from the fact that eqn. (22) is derived by equating eqn. (19) to eqn. (20). As both S and $p_d - p_n$ are positive (or zero) and J is negative (see Fig. 2), the very derivation of eqn. (22) and hence of eqns. (27) and (28) implies $(\mathrm{d}p/\mathrm{d}x)|_{x=d} \leqslant 0$.

5. Special cases and applications

5.1. Effect of the back-surface field on J_{sc}

When a p$^+$–n–n$^+$ cell operates under short-circuit conditions,

$$p_0 \to p_n$$

and

$$J_R \to J_{sc}$$

Under these conditions, eqn. (28) gives

$$J_{scb_l} = qD_p\left[\sum \frac{N_0}{L_\lambda}\exp\left(-\frac{d_p + d_s}{L_\lambda}\right) + \right.$$
$$\left. + \frac{\epsilon\,\mathrm{sech}(d/L)}{L\{1 + \epsilon\tanh(d/L)\}}\sum N_0\exp\left(-\frac{w}{L_\lambda}\right)\right] -$$
$$-qD_p\left[\frac{\epsilon + \tanh(d/L)}{L\{1 + \epsilon\tanh(d/L)\}}\sum N_0\exp\left(-\frac{d_p + d_s}{L_\lambda}\right) + \right.$$
$$\left. + \frac{\mathrm{sech}(d/L)}{1 + \epsilon\tanh(d/L)}\sum\frac{N_0}{L_\lambda}\exp\left(-\frac{w}{L_\lambda}\right)\right] \qquad (30)$$

For most cases in practice where the thickness w of silicon solar cells is greater than 100 μm and the cell is illuminated with sunlight, the terms containing $\exp(-w/L_\lambda)$ in eqn. (30) are usually negligible. For such a case, eqn. (30) can be approximated to

$$J_{scb_l} \approx qD_p\left[\sum\frac{N_0}{L_\lambda}\exp\left(-\frac{d_p + d_s}{L_\lambda}\right) - \right.$$
$$\left. - \frac{\epsilon + \tanh(d/L)}{L\{1 + \epsilon\tanh(d/L)\}}\sum N_0\exp\left(-\frac{d_p + d_s}{L_\lambda}\right)\right] \qquad (31)$$

Without a BSF, $S = \infty$, *i.e.* $\epsilon = \infty$, and eqn. (31) represents the case of a conventional p$^+$–n cell and J_{scc_l} is obtained from eqn. (31) as

$$J_{scc_l} \approx qD_p\left\{\sum\frac{N_0}{L_\lambda}\exp\left(-\frac{d_p + d_s}{L_\lambda}\right) - \frac{\coth(d/L)}{L}\sum N_0\exp\left(-\frac{d_p + d_s}{L_\lambda}\right)\right\} \qquad (32)$$

Subtracting eqn. (32) from eqn. (31) the improvement in J_{sc} due to the BSF (*i.e.* ΔJ_{sc}) can be obtained as

$$\Delta J_{sc} \approx \frac{\coth(d/L) - \tanh(d/L)}{L\{1 + \epsilon \tanh(d/L)\}} \sum N_0 \exp\left(-\frac{d_p + d_s}{L_\lambda}\right) \tag{33}$$

Substituting eqn. (16) into eqn. (33)

$$\Delta J_{sc} \approx \frac{\coth(d/L) - \tanh(d/L)}{1 + \epsilon \tanh(d/L)} \sum \frac{q(1 - R_\lambda)n_{ph}LL_\lambda}{L^2 - L_\lambda{}^2} \exp\left(-\frac{d_p + d_s}{L_\lambda}\right) \tag{34}$$

It may be emphasized that, unlike eqns. (31) and (32), eqn. (34) may be valid even if the contributions of the front region and the space charge layer at the front junction to the total short-circuit current density are not negligible compared with the contribution of the bulk region.

From eqn. (34), the following points can be noted.

(1) There is almost no improvement in the short-circuit current density due to the BSF if $d/L > 3$. However, a cell with a smaller d/L will have a larger improvement in J_{sc}. This improvement is maximum when $\epsilon = 0$.

(2) ΔJ_{sc} will be higher for radiations with smaller absorption coefficients (*i.e.* for larger L_λ since $\alpha_\lambda = L_\lambda{}^{-1}$).

(3) ΔJ_{sc} will improve for a reduction in R_λ and for an increase in the incident photon flux.

5.2. *Open-circuit voltages of back-surface field cells*

The open-circuit voltage of a p^+–n–n^+ cell can be given by

$$V_{ocb_1} = V_{J_{oc}} + V_{n_{oc}} + V_{nn^+{}_{oc}} \tag{35}$$

where $V_{n_{oc}}$ is the photovoltage across the bulk n region for open-circuit conditions, $V_{nn^+{}_{oc}}$ is the photovoltage developed at the n–n^+ back junction for open-circuit conditions, and $V_{J_{oc}}$, $V_{n_{oc}}$ and $V_{nn^+{}_{oc}}$ are given by the following equations:

$$V_{J_{oc}} = \frac{kT}{q} \ln\left(\frac{p_{Ob_1}}{p_n}\right) \tag{36}$$

$$V_{n_{oc}} = \frac{b - 1}{b + 1}\frac{kT}{q} \ln\left(\frac{N_D + p_{Ob_1}}{N_D + p_{d_1}}\right) \tag{37}$$

$$V_{nn^+{}_{oc}} = \frac{kT}{q} \ln\left(\frac{N_D + p_{d_1}}{N_D + p_n}\right) \tag{38}$$

$V_{n_{oc}}$ is due to the Dember potential. The Dember potential [26] owes its origin to the unequal diffusion coefficients of electrons and holes in a semiconductor; it is able to develop across the bulk region of a cell for high level conditions if the carrier densities at the two ends of the bulk region are unequal. Because electrons have a higher mobility than holes, the polarity of the Dember voltage is such that the higher carrier density end of the bulk region of each p/n and n/p (BSF or conventional) silicon cell is positive with respect to the lower carrier density end [27]. As a result the Dember voltage is additive to the photovoltage of a p/n cell if the carrier density is higher on the p^+–n junction end of the bulk region. However, the Dember voltage would be additive to the photovoltage of an n/p cell if the carrier density is higher at the p–p^+ junction end of the bulk region. Therefore the Dember voltage is a useful photovoltage for a p/n conventional cell whereas it is detrimental to an n/p conventional cell. V_{nn^+oc} is negligible for low level conditions and can be appreciable for high level conditions provided that $p_{d_1} \gg N_D$.

The substitution of eqns. (36) - (38) into eqn. (35) yields

$$V_{ocb_1} = \frac{kT}{q} \ln\left(\frac{p_{0b_1}}{p_n}\right) + \frac{b-1}{b+1}\frac{kT}{q} \ln\left(1 + \frac{p_{0b_1}}{N_D}\right) + $$

$$+ \frac{2}{b+1}\frac{kT}{q} \ln\left(1 + \frac{p_{d_1}}{N_D}\right) \tag{39a}$$

where $p_n \ll N_D$.

In contrast, the open-circuit voltage of an n^+–p–p^+ cell is given by

$$V_{ocb_2} = \frac{kT}{q} \ln\left(\frac{n_{0b_2}}{n_p}\right) - \frac{b-1}{b+1}\frac{kT}{q} \ln\left(1 + \frac{n_{0b_2}}{N_A}\right) + $$

$$+ \frac{2b}{b+1}\frac{kT}{q} \ln\left(1 + \frac{n_{d_2}}{N_A}\right) \tag{39b}$$

where $n_p \ll N_A$.

It is interesting to note that eqn. (39b) can be obtained straight away from eqn. (39a) by replacing b by b^{-1} and writing it for an n^+–p–p^+ cell.

Equations (39a) and (39b) give general expressions for V_{ocb_1} and V_{ocb_2} and cases of low and high level conditions can be discussed from them.

5.2.1. Low level conditions

For low level conditions in the bulk region of a p/n BSF cell

$$p_{0b_1}/N_D \ll 1 \qquad \text{and} \qquad p_{d_1}/N_D \ll 1$$

For such a case, eqn. (39a) yields

$$V_{ocbl_1} \approx \frac{kT}{q} \ln\left(\frac{p_{0b_1}}{p_n}\right) \tag{40}$$

Then

$$V_{ocbl_1} \approx V_{J_{ocb_1}} \tag{41}$$

For open-circuit conditions the combination of eqns. (6), (27), (28) and (30) gives p_{0b_1} as

$$p_{0b_1} = \frac{J_{scb_1} L\{1 + \epsilon \tanh(d/L)\}}{qD_p\{\epsilon + \tanh(d/L)\}} \tag{42}$$

where $p_{0b_1} \gg p_n$.

Equation (42) in conjunction with eqn. (40) gives

$$V_{\mathrm{ocbl}_1} = \frac{kT}{q} \ln \left[\frac{J_{\mathrm{scb}_1} L\{1 + \epsilon \tanh(d/L)\}}{q D_{\mathrm{p}} p_{\mathrm{n}} \{\epsilon + \tanh(d/L)\}} \right] \tag{43}$$

In terms of the bulk resistivity ρ_{B}, eqn. (43) can be written as

$$V_{\mathrm{ocbl}_1} = \frac{kT}{q} \ln \left[\frac{kT J_{\mathrm{scb}_1} L\{1 + \epsilon \tanh(d/L)\}}{q^3 n_{\mathrm{i}}^2 D_{\mathrm{p}} D_{\mathrm{n}} \rho_{\mathrm{B}} \{\epsilon + \tanh(d/L)\}} \right] \tag{44a}$$

Similarly for an n^+–p–p^+ cell we can obtain

$$V_{\mathrm{ocbl}_2} = \frac{kT}{q} \ln \left[\frac{kT J_{\mathrm{scb}_2} L\{1 + \epsilon \tanh(d/L)\}}{q^3 n_{\mathrm{i}}^2 D_{\mathrm{p}} D_{\mathrm{n}} \rho_{\mathrm{B}} \{\epsilon + \tanh(d/L)\}} \right] \tag{44b}$$

A comparison of eqns. (44a) and (44b) shows that, if $J_{\mathrm{scb}_1} = J_{\mathrm{scb}_2}$, and d, L and ρ_{B} are the same for p^+–n–n^+ and n^+–p–p^+ cells, then the two cells can show equal open-circuit voltages for low level conditions.

V_{ocbl} will increase with an increase in J_{sc} and L and with a decrease in ϵ and ρ_{B}.

5.2.2. High level conditions

For high level conditions in the bulk region,

$$p_{\mathrm{0b}_1}/N_{\mathrm{D}} \gg 1 \qquad \text{and} \qquad p_{d_1}/N_{\mathrm{D}} \gg 1$$

Hence, eqn. (39a) reduces to

$$V_{\mathrm{ocbh}_1} = \frac{2kT}{q} \ln\left(\frac{p_{\mathrm{0b}_1}}{n_{\mathrm{i}}}\right) + \frac{2}{b+1} \frac{kT}{q} \ln\left(\frac{p_{d_1}}{p_{\mathrm{0b}_1}}\right) \tag{45a}$$

For an n^+–p–p^+ cell, however, V_{ocbh_2} would be given by

$$V_{\mathrm{ocbh}_2} = \frac{2kT}{q} \ln\left(\frac{n_{\mathrm{0b}_2}}{n_{\mathrm{i}}}\right) + \frac{2b}{b+1} \frac{kT}{q} \ln\left(\frac{n_{d_2}}{n_{\mathrm{0b}_2}}\right) \tag{45b}$$

For $(\mathrm{d}p/\mathrm{d}x)|_{x=d} \leqslant 0$, the substitution of eqn. (42) into eqn. (45a) gives

$$V_{\mathrm{ocbh}_1} = \frac{2kT}{q} \ln \left[\frac{J_{\mathrm{scb}_1} L\{1 + \epsilon \tanh(d/L)\}}{q D_{\mathrm{p}} n_{\mathrm{i}} \{\epsilon + \tanh(d/L)\}} \right] + \frac{2}{b+1} \frac{kT}{q} \ln\left(\frac{p_{d_1}}{p_{\mathrm{0b}_1}}\right) \tag{46a}$$

Similarly, for an n^+–p–p^+ cell, eqn. (45b) gives

$$V_{\mathrm{ocbh}_2} = \frac{2kT}{q} \ln \left[\frac{J_{\mathrm{scb}_2} L\{1 + \epsilon \tanh(d/L)\}}{q D_{\mathrm{n}} n_{\mathrm{i}} \{\epsilon + \tanh(d/L)\}} \right] + \frac{2b}{b+1} \frac{kT}{q} \ln\left(\frac{n_{d_2}}{n_{\mathrm{0b}_2}}\right) \tag{46b}$$

Also, for most front-illuminated p^+–n–n^+ silicon solar cells in sunlight, p_{d_1} may be given approximately from eqn. (25) as

$$p_{d_1} \approx \frac{[p_{0b_1} + \Sigma N_0 \exp\{-(d_p + d_s)/L_\lambda\}]\ \mathrm{sech}(d/L)}{1 + \epsilon\ \tanh(d/L)} \tag{47a}$$

This is because generally for silicon solar cells, in practice, $w > 100\ \mu$m, *i.e.* $w \gg (d_p + d_s)$, and this makes the second and the third term in the numerator on the right-hand side of eqn. (25) negligible compared with the first term.

Similarly for most front-illuminated n^+–p–p^+ silicon solar cells in practice

$$n_{d_2} \approx \frac{[n_{0b_2} + \Sigma N_0 \exp\{-(d_p + d_s)/L_\lambda\}]\ \mathrm{sech}(d/L)}{1 + \epsilon\ \tanh(d/L)} \tag{47b}$$

Equation (42) shows that p_{0b_1} is large when L is large and $\epsilon \to 0$. For such cases, eqn. (47a) may be reduced to

$$p_{d_1} \approx \frac{p_{0b_1}\ \mathrm{sech}(d/L)}{1 + \epsilon\ \tanh(d/L)} \tag{48a}$$

Similarly, eqn. (47b) may give

$$n_{d_2} \approx \frac{n_{0b_2}\ \mathrm{sech}(d/L)}{1 + \epsilon\ \tanh(d/L)} \tag{48b}$$

It may be mentioned that in further discussions we shall limit ourselves to eqns. (48a) and (48b). For exact computation we may use eqns. (47a) and (47b).

Combining eqn. (46a) with eqn. (48a) and eqn. (46b) with eqn. (48b), V_{ocbh_1} and V_{ocbh_2} can be expressed as

$$V_{\mathrm{ocbh}_1} = \frac{2kT}{q} \ln\left[\frac{J_{\mathrm{scb}_1} L\{1 + \epsilon\ \tanh(d/L)\}}{qD_p n_i\{\epsilon + \tanh(d/L)\}}\right] + \frac{2}{b+1}\frac{kT}{q} \ln\left\{\frac{\mathrm{sech}(d/L)}{1 + \epsilon\ \tanh(d/L)}\right\} \tag{49a}$$

and

$$V_{\mathrm{ocbh}_2} = \frac{2kT}{q} \ln\left[\frac{J_{\mathrm{scb}_2} L\{1 + \epsilon\ \tanh(d/L)\}}{qD_n n_i\{\epsilon + \tanh(d/L)\}}\right] + \frac{2b}{b+1}\frac{kT}{q} \ln\left\{\frac{\mathrm{sech}(d/L)}{1 + \epsilon\ \tanh(d/L)}\right\} \tag{49b}$$

Equations (49a) and (49b) show that for high level conditions the open-circuit voltage of BSF cells is independent of ρ_B. This has been found in practice also. Both 10 and 100 Ω cm resistivity p^+–n–n^+ silicon solar cells have exhibited an open-circuit voltage of about 0.6 V at 27 °C under an intensity of illumination of 1 sun [3, 4]. Similarly, both 10 and 100 Ω cm resistivity n^+–p–p^+ silicon solar cells have shown an open-circuit voltage of about 0.6 V at 25 °C under an intensity of illumination of 1 sun [2]. Equations (49a) and (49b) further show that, if $J_{\mathrm{scb}_1} = J_{\mathrm{scb}_2}$ and L is also the same for p$^+$–n–n$^+$ and n$^+$–p–p$^+$ cells, then for $\epsilon \to 0$ and $d/L \ll 1$

$$V_{\mathrm{ocbh}_1} - V_{\mathrm{ocbh}_2} \approx \frac{2kT}{q} \ln b \tag{50}$$

For silicon cells, as $b = 2.8$, eqn. (50) shows that, at room temperature where $kT/q \approx 25$ mV, $V_{\mathrm{ocbh}_1} - V_{\mathrm{ocbh}_2} \approx 50$ mV. This is in agreement with the results of Fossum *et al.* [15] and Wu and Shen [16]. A comparison of eqns. (49a), (49b) and (50) shows that $V_{\mathrm{ocbh}_1} - V_{\mathrm{ocbh}_2}$ increases further with an increase in d/L or ϵ, because the BSF effect decreases with an increase in d/L or ϵ.

It may be pointed out that the experimental data [2 - 4] on 10 Ω cm and more significantly on 100 Ω cm resistivity p$^+$–n–n$^+$ and n$^+$–p–p$^+$ silicon solar cells, as referred to above in the context of the independence of V_{ocbh_1} and V_{ocbh_2} on ρ_{B}, do not show a difference of about 50 mV between V_{ocbh_1} and V_{ocbh_2} at room temperature. On the contrary, these data show that the open-circuit voltages of p$^+$–n–n$^+$ and n$^+$–p–p$^+$ cells with $d/L \ll 1$ may be nearly equal for high level conditions.

The present analysis reveals that for $d/L \ll 1$ the difference of about 50 mV has its origin in the assumption that $(\mathrm{d}p/\mathrm{d}x)|_{x=d} \leqslant 0$ for both p$^+$–n–n$^+$ and n$^+$–p–p$^+$ cells. The validity of $(\mathrm{d}p/\mathrm{d}x)|_{x=d} \leqslant 0$ for these cells will be discussed later.

5.3. Open-circuit voltage of conventional cells

For a p$^+$–n cell, since $\epsilon \approx \infty$, eqn. (39a) reduces to

$$V_{\mathrm{occ}_1} = \frac{kT}{q} \ln\left(\frac{p_{0\mathrm{c}_1}}{p_{\mathrm{n}}}\right) + \frac{b-1}{b+1}\,\frac{kT}{q} \ln\left(1 + \frac{p_{0\mathrm{c}_1}}{N_{\mathrm{D}}}\right) \tag{51a}$$

Similarly, for an n$^+$–p cell, eqn. (39b) gives

$$V_{\mathrm{occ}_2} = \frac{kT}{q} \ln\left(\frac{n_{0\mathrm{c}_2}}{n_{\mathrm{p}}}\right) - \frac{b-1}{b+1}\,\frac{kT}{q} \ln\left(1 + \frac{n_{0\mathrm{c}_2}}{N_{\mathrm{A}}}\right) \tag{51b}$$

For low level conditions, $p_{0\mathrm{c}_1}/N_{\mathrm{D}} \ll 1$ and $n_{0\mathrm{c}_2}/N_{\mathrm{A}} \ll 1$. Therefore, for low level conditions, eqns. (51a) and (51b) give

$$V_{\mathrm{occl}_1} = \frac{kT}{q} \ln\left\{\frac{kTJ_{\mathrm{scc}_1}L\tanh(d/L)}{q^3 n_{\mathrm{i}}^2 D_{\mathrm{p}} D_{\mathrm{n}} \rho_{\mathrm{B}}}\right\} \tag{52a}$$

and

$$V_{\mathrm{occl}_2} = \frac{kT}{q} \ln\left\{\frac{kTJ_{\mathrm{scc}_2}L\tanh(d/L)}{q^3 n_{\mathrm{i}}^2 D_{\mathrm{p}} D_{\mathrm{n}} \rho_{\mathrm{B}}}\right\} \tag{52b}$$

respectively.

Equations (52a) and (52b) show that under low level conditions the open-circuit voltages of p$^+$–n and n$^+$–p conventional cells are equal if J_{sc}, L, d and ρ_{B} are the same for the two cells.

For high level conditions, eqn. (51a) yields

$$V_{\mathrm{occh}_1} = \frac{kT}{q} \ln\left\{\frac{kTJ_{\mathrm{scc}_1}L \tanh(d/L)}{q^3 n_i^{\,2} D_p D_n \rho_B}\right\} + $$

$$+ \frac{b-1}{b+1}\,\frac{kT}{q} \ln\left\{\frac{qJ_{\mathrm{scc}_1} bL\rho_B \tanh(d/L)}{kT}\right\} \tag{53a}$$

and eqn. (51b) yields

$$V_{\mathrm{occh}_2} = \frac{kT}{q} \ln\left\{\frac{kTJ_{\mathrm{scc}_2}L \tanh(d/L)}{q^3 n_i^{\,2} D_p D_n \rho_B}\right\} - $$

$$- \frac{b-1}{b+1}\,\frac{kT}{q} \ln\left\{\frac{qJ_{\mathrm{scc}_2} L\rho_B \tanh(d/L)}{bkT}\right\} \tag{53b}$$

In eqn. (53a), both the terms on the right-hand side are positive whereas in eqn. (53b) the second term is negative. Equations (53a) and (53b) thus show that for high level conditions the open-circuit voltage of a p^+–n cell will be higher than that of an n^+–p cell if ρ_B is the same for both of them. Also, V_{occh_1} would increase much more rapidly with J_{scc_1} (or the intensity of illumination) than would V_{occh_2} for a similar increase in J_{scc_2}. This has been corroborated experimentally [15].

5.4. *Improvement in open-circuit voltage due to the back-surface field effect*

ΔV_{oc_1} can be computed as

$$\Delta V_{\mathrm{oc}_1} = V_{\mathrm{ocb}_1} - V_{\mathrm{occ}_1} \tag{54}$$

The substitution of eqns. (39a) and (51a) in eqn. (54) gives

$$\Delta V_{\mathrm{oc}_1} = \frac{kT}{q} \ln\left(\frac{p_{\mathrm{ob}_1}}{p_{\mathrm{oc}_1}}\right) + \frac{b-1}{b+1}\,\frac{kT}{q} \ln\left(1 + \frac{p_{\mathrm{ob}_1}}{N_D}\right) - $$

$$- \frac{b-1}{b+1}\,\frac{kT}{q} \ln\left(1 + \frac{p_{\mathrm{oc}_1}}{N_D}\right) + $$

$$+ \frac{2}{b+1}\,\frac{kT}{q} \ln\left(1 + \frac{p_{d_1}}{N_D}\right) \tag{55}$$

Expressing

$$\Delta V_{\mathrm{J_{oc}}_1} = V_{\mathrm{J_{ocb}}_1} - V_{\mathrm{J_{occ}}_1} \tag{56}$$

and substituting the equations

$$p_{\mathrm{ob}_1} = p_n \exp\left(\frac{qV_{\mathrm{J_{ocb}}_1}}{kT}\right) \tag{57a}$$

and

$$p_{0c_1} = p_n \exp\left(\frac{qV_{J_{occ_1}}}{kT}\right) \tag{57b}$$

we can write

$$\Delta V_{J_{oc_1}} = \frac{kT}{q} \ln\left(\frac{p_{0b_1}}{p_{0c_1}}\right) \tag{58}$$

Substituting $\epsilon = \infty$ in eqn. (42), p_{0c_1} is obtained as

$$p_{0c_1} = \frac{J_{scc_1} L \tanh(d/L)}{qD_p} \tag{59}$$

Dividing eqn. (42) by eqn. (59) we can obtain

$$\frac{p_{0b_1}}{p_{0c_1}} = \frac{J_{scb_1}}{J_{scc_1}} \frac{\epsilon + \coth(d/L)}{\epsilon + \tanh(d/L)} \tag{60}$$

The substitution of eqn. (60) into eqn. (58) gives

$$\Delta V_{J_{oc_1}} = \frac{kT}{q} \ln\left\{\frac{J_{scb_1}}{J_{scc_1}} \frac{\epsilon + \coth(d/L)}{\epsilon + \tanh(d/L)}\right\} \tag{61}$$

Equations (55) and (60) give

$$\begin{aligned} \Delta V_{oc_1} = {} & \frac{kT}{q} \ln\left\{\frac{J_{scb_1}}{J_{scc_1}} \frac{\epsilon + \coth(d/L)}{\epsilon + \tanh(d/L)}\right\} + \\ & + \frac{b-1}{b+1}\frac{kT}{q} \ln\left(1 + \frac{p_{0b_1}}{N_D}\right) - \\ & - \frac{b-1}{b+1}\frac{kT}{q} \ln\left(1 + \frac{p_{0c_1}}{N_D}\right) + \\ & + \frac{2}{b+1}\frac{kT}{q} \ln\left(1 + \frac{p_{d_1}}{N_D}\right) \end{aligned} \tag{62a}$$

For an n^+–p–p^+ cell, however, we obtain

$$\begin{aligned} \Delta V_{oc_2} = {} & \frac{kT}{q} \ln\left\{\frac{J_{scb_2}}{J_{scc_2}} \frac{\epsilon + \coth(d/L)}{\epsilon + \tanh(d/L)}\right\} - \\ & - \frac{b-1}{b+1}\frac{kT}{q} \ln\left(1 + \frac{n_{0b_2}}{N_A}\right) + \\ & + \frac{b-1}{b+1}\frac{kT}{q} \ln\left(1 + \frac{n_{0c_2}}{N_A}\right) + \\ & + \frac{2b}{b+1}\frac{kT}{q} \ln\left(1 + \frac{n_{d_2}}{N_A}\right) \end{aligned} \tag{62b}$$

Equations (62a) and (62b) are quite general in nature. However, the following two cases are of special interest: (i) when both BSF and conventional cells are under low level conditions; (ii) when both BSF and conventional cells are under high level conditions.

5.4.1. Case (i)

For low level conditions in the bulk region of both p^+–n–n^+ and p^+–n cells, since $p_{0b_1}/N_D \ll 1$, $p_{0c_1}/N_D \ll 1$ and $p_{d_1}/N_D \ll 1$, eqn. (62a) reduces to

$$\Delta V_{ocl_1} = \frac{kT}{q} \ln \left\{ \frac{J_{scb_1}}{J_{scc_1}} \frac{\epsilon + \coth(d/L)}{\epsilon + \tanh(d/L)} \right\} \tag{63}$$

A similar equation can be written for an n^+–p–p^+ cell. Therefore, for low level conditions, in general, we can write

$$\Delta V_{ocl} = \frac{kT}{q} \ln\left(\frac{J_{scb}}{J_{scc}}\right) + \frac{kT}{q} \ln \left\{ \frac{\epsilon + \coth(d/L)}{\epsilon + \tanh(d/L)} \right\} \tag{64}$$

In practice [3], $J_{scb}/J_{scc} \approx 1.1$; hence any significant value of ΔV_{ocl} is due to the second term in eqn. (64). ΔV_{ocl} is independent of ρ_B and depends on ϵ and d/L. This shows that, if ϵ and d/L are the same for p/n BSF and n/p BSF cells, then ΔV_{ocl} is the same for them both.

ΔV_{ocl} is a maximum for $\epsilon = 0$ and is given by

$$\Delta V_{ocl} = \frac{kT}{q} \ln\left(\frac{J_{scb}}{J_{scc}}\right) + \frac{2kT}{q} \ln \left\{ \coth\left(\frac{d}{L}\right) \right\} \tag{65}$$

Since the contribution of the first term on the right-hand side is usually negligible, ΔV_{ocl} is very small if $d/L \geqslant 3$. It shows that, as Godlewski *et al.* [8] found, an insignificant improvement in V_{oc} for $d/L > 3$ occurs for both p^+–n–n^+ and n^+–p–p^+ cells, provided that the cells operate under low level conditions.

A comparison of eqns. (63) and (61) shows that

$$\Delta V_{ocl_1} \approx \Delta V_{J_{oc_1}} \tag{66}$$

Similarly, for an n/p BSF cell,

$$\Delta V_{ocl_2} \approx \Delta V_{J_{oc_2}} \tag{67}$$

Equations (66) and (67) show that for low level conditions the improvement in the open-circuit voltage due to a BSF arises because an additional photovoltage is developed at the p–n junction. It has its origin in the back reflection of minority carriers, which accounts for the increase in the minority carrier density at the p–n front-junction end of the bulk region from p_{0c_1} to p_{0b_1} and from n_{0c_2} to n_{0b_2} for p/n and n/p BSF cells respectively.

Figure 3 shows the dependence of ΔV_{ocl} on d/L with ϵ as the parameter. Equation (63) was used to compute ΔV_{ocl} on the assumptions that kT/q = 0.02587 V and J_{scb}/J_{scc} = 1.1. As can be seen from eqn. (34), $\Delta J_{sc} \to 0$ for $\epsilon \to \infty$ or $d/L > 3$, and hence the assumption that J_{scb}/J_{scc} = 1.1 does not hold for $\epsilon \to \infty$. This correction was not applied in plotting the curves in

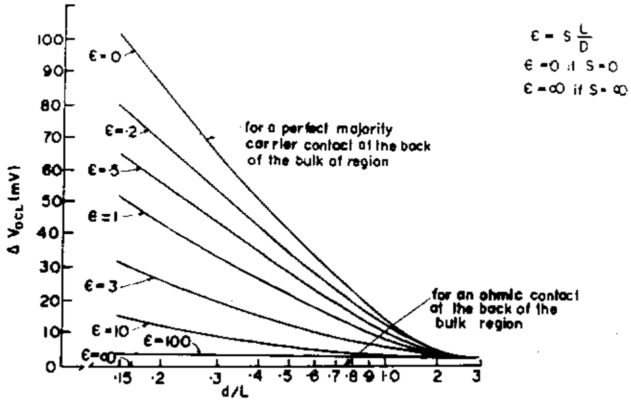

Fig. 3. ΔV_{oc} for low level conditions in the bulk region of a BSF solar cell at T = 27 °C (300 K) as a function of d/L with ϵ as parameter. $\epsilon = 0$ stands for a perfect minority-carrier-blocking L–H junction contact at $x = d$, $\epsilon > 0$ signifies imperfect blocking and $\epsilon = \infty$ represents an ohmic contact at $x = d$. The curves are valid for both p/n and n/p BSF cells of silicon and may be valid for cells of other semiconductors also.

Fig. 3 and this is why ΔV_{ocl} for $\epsilon = 100$ and $d/L \approx 3.0$ is not zero (practically) and is 2.4 mV instead. If we neglect this, it can be observed that ΔV_{ocl} is practically zero for $d/L \geqslant 2.5$ or $\epsilon \geqslant 100$. In general, ΔV_{ocl} is higher for a smaller d/L or a smaller ϵ.

For minority carrier MIS silicon cells with a p–p$^+$ L–H junction at the back surface and d = 300 μm, L = 800 μm (*i.e.* d/L = 0.375) and ρ_B = 10 Ω cm, Tarr *et al.* [28] have observed an increase in V_{oc} from 0.54 to 0.59 V at room temperature. This value of ΔV_{oc} is in excellent agreement with the theoretical ΔV_{oc}, as shown in Fig. 3 for $\epsilon = 0$. It shows that Fig. 3 may be valid for p–n junction-like MIS BSF cells also.

5.4.2. Case (ii)

For high level conditions in the bulk regions of both p$^+$–n–n$^+$ and p$^+$–n cells,

$$p_{0b_1}/N_D \gg 1 \qquad p_{0c_1}/N_D \gg 1 \qquad p_{d_1}/N_D \gg 1$$

Under these conditions, eqn. (54) in conjunction with eqn. (57b) yields

$$\Delta V_{och_1} = \frac{2b}{b+1}\Delta V_{J_{oc_1}} + \frac{2}{b+1}\frac{kT}{q}\ln\left(\frac{p_{d_1}}{N_D}\right) \tag{68a}$$

Similarly, for an n/p BSF cell,

$$\Delta V_{och_2} = \frac{2}{b+1}\Delta V_{J_{oc_2}} + \frac{2b}{b+1}\frac{kT}{q}\ln\left(\frac{n_{d_2}}{N_A}\right) \tag{68b}$$

An immediate conclusion drawn from a comparison of eqns. (68a) and (68b) is that, even if the ΔV_{oc} values are equal for p/n and n/p BSF cells for low level conditions, they would normally be different for high level conditions. p_{d_1}/N_D can be determined from eqns. (42) and (48a) as

$$\frac{p_{d_1}}{N_{\mathrm{D}}} = \frac{qJ_{\mathrm{scb}_1}bL\rho_{\mathrm{B}}\,\mathrm{sech}(d/L)}{kT\{\epsilon + \tanh(d/L)\}} \tag{69a}$$

Similarly, n_{d_2}/N_{A} can be obtained as

$$\frac{n_{d_2}}{N_{\mathrm{A}}} = \frac{qJ_{\mathrm{scb}_2}L\rho_{\mathrm{B}}\,\mathrm{sech}(d/L)}{bkT\{\epsilon + \tanh(d/L)\}} \tag{69b}$$

As discussed under case (i), $\Delta V_{\mathrm{J}_{\mathrm{oc}_1}}$ and $\Delta V_{\mathrm{J}_{\mathrm{oc}_2}}$ are nearly independent of ρ_{B} and the intensity of illumination. Therefore, the first term on the right-hand side of eqn. (68a) and the first term on the right-hand side of eqn. (68b) would be independent of ρ_{B} and the intensity of illumination. However, as shown by eqns. (69a) and (69b) the second term on the right-hand side of eqn. (68a) and the second term on the right-hand side of eqn. (68b) would increase with both ρ_{B} and J_{sc} (or with the intensity of illumination). Also it should be noted that the increase in the second term of eqn. (68a) with ρ_{B} and J_{sc} would be b times the increase in the second term of eqn. (68b).

A very important conclusion drawn here is that, if the second term dominates the first term in eqn. (68a) and if the second term dominates the first term in eqn. (68b), an n^+–p–p^+ cell would show a larger improvement in open-circuit voltage due to the BSF than that shown by a p^+–n–n^+ cell.

The origin of the second term lies in the ability of the BSF at the L–H back junction to block the transport of minority carriers from the bulk region to the back n^+ and p^+ regions of the p^+–n–n^+ and n^+–p–p^+ cells respectively and thereby to cause an increase (due to the requirement of approximate space charge neutrality) in the majority carrier density significantly above the thermal equilibrium value at the L–H junction end of the bulk region.

At first sight it appears that the first term in eqn. (68a) and the first term in eqn. (68b) should owe their existence to the back-reflection property of the BSF and the second term in eqn. (68a) and the second term in eqn. (68b) to the blocking capability of the BSF; while the contribution of back reflection is greater for a p/n BSF cell, the contribution of minority carrier blocking is greater for an n/p BSF cell. This point will be discussed further in Section 6.

In addition to the above cases (i) and (ii) the equations can be used to determine ΔV_{oc} for a general case where low and high level conditions may not be too well defined. For p/n BSF cells, eqn. (62a) can then be used in conjunction with

$$\frac{p_{0\mathrm{b}_1}}{N_{\mathrm{D}}} = \frac{qJ_{\mathrm{scb}_1}bL\rho_{\mathrm{B}}\{1 + \epsilon\tanh(d/L)\}}{kT\{\epsilon + \tanh(d/L)\}} \tag{70}$$

$$\frac{p_{0\mathrm{c}_1}}{N_{\mathrm{D}}} = \frac{qJ_{\mathrm{scc}_1}bL\rho_{\mathrm{B}}\tanh(d/L)}{kT} \tag{71}$$

and eqn. (69a).

For an n/p BSF cell, eqn. (62b) can then be used in conjunction with

$$\frac{n_{0\mathrm{b}_2}}{N_\mathrm{A}} = \frac{qJ_{\mathrm{scb}_2}L\rho_\mathrm{B}\{1+\epsilon\tanh(d/L)\}}{bkT\{\epsilon+\tanh(d/L)\}} \tag{72}$$

$$\frac{n_{0\mathrm{c}_1}}{N_\mathrm{A}} = \frac{qJ_{\mathrm{scc}_1}L\rho_\mathrm{B}\tanh(d/L)}{bkT} \tag{73}$$

and eqn. (69b).

6. Development of $\Delta V_{\mathrm{och}_1}$ and $\Delta V_{\mathrm{och}_2}$

In order to analyse the effect of the BSF on the open-circuit voltages of front-illuminated p^+–n–n^+ and n^+–p–p^+ cells for high level conditions in their bulk regions, let us assume that the n–n^+ and p–p^+ junctions are added to the backs of the front-illuminated conventional p^+–n and n^+–p cells respectively which are already in the open-circuit condition and have an electric field due to the Dember potential in their bulk regions. Figures 4(a) and 4(b) respectively show initial electron and hole flows in the bulk regions of p^+–n–n^+ and n^+–p–p^+ cells thus formed.

For a p^+–n–n^+ cell (Fig. (4a)), holes flowing under a field as well as by diffusion face a blocking barrier in the newly added n–n^+ junction and pile up at $x = d$. The piling-up of holes at $x = d$ also decreases the magnitude of the concentration gradient of holes at $x = 0$, *i.e.* $(\mathrm{d}p/\mathrm{d}x)|_{x=0}$ is reduced. This in turn tries to reduce the dark current density J_d. For electrons flowing by diffusion, the n–n^+ junction acts as a collector junction and increases the radiation current density J_R. Both these events force the p^+ emitter to inject more holes into the n region to maintain $J_\mathrm{R} = J_d$ (or $J = 0$, the zero-current

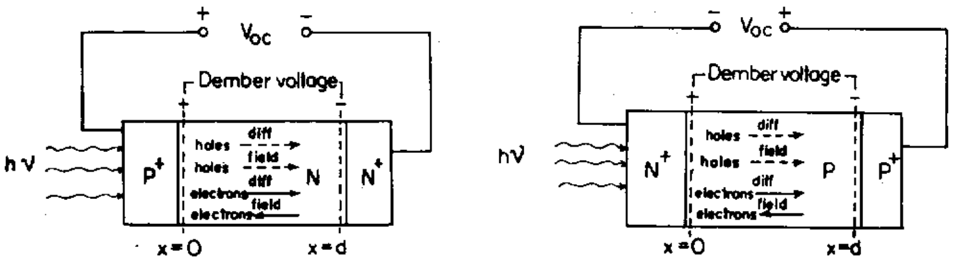

(a) (b)

Fig. 4. Carrier transport mechanisms in the bulk region in the presence of an electric field due to the Dember voltage for high level conditions in the bulk regions of front-illuminated p^+–n–n^+ and n^+–p–p^+ silicon solar cells at open circuit: (a) a p^+–n–n^+ cell; (b) an n^+–p–p^+ cell. The Dember voltage shown in each case corresponds to the p^+–n and n^+–p cells (already at open circuit) prior to the addition of the n^+ and p^+ regions at the back of the p^+–n and n^+–p cells respectively.

condition) in the open circuit. It is essential that quasi-neutrality in the bulk region, as given by $dn/dx \approx dp/dx$ and $n \approx p + N_D$, be maintained throughout. For the low level conditions in the bulk n region, the above requirement is easily met owing to the availability of a large number of electrons throughout the bulk region. However, for high level conditions in the bulk region, the necessary number of electrons can be supplied by the n^+ region only. Therefore the n^+ emitter injects electrons into the bulk n region. This leads to an increase in carrier density in the n region at both $x = 0$ and $x = d$. It must be emphasized here that initially the increase in carrier density at $x = 0$ is preferred because of a favourable field in the n region which sweeps electrons from $x = d$ towards the p^+–n junction at $x = 0$ and is realized in practice because the p^+–n junction is able to block the transport of electrons from the bulk n region to the p^+ side. An increased carrier density at $x = 0$ leads to the development of an additional photovoltage $\Delta V_{J_{oc_1}}$ at the p^+–n (p–n) junction and the increased carrier density at $x = d$ generates an additional photovoltage

$$V_{nn^+oc} = \frac{kT}{q} \ln\left(\frac{n_{d_1}}{N_D}\right)$$

at the n–n^+ (L–H) junction. The contribution of the bulk region to the photovoltage is also modified. The increased carrier density at $x = 0$ attempts to increase the Dember potential by $\{(b-1)/(b+1)\}\Delta V_{J_{oc_1}}$. However, the increased carrier density at $x = d$ attempts to decrease the Dember potential by $\{(b-1)/(b+1)\}V_{nn^+oc}$. Since the Dember voltage is additive to the photovoltage of a p^+–n cell, the net improvement in the open-circuit voltage due to the addition of an n^+ layer at the back is given for high level conditions in the bulk n region as

$$\Delta V_{och_1} = \Delta V_{J_{oc_1}} + \frac{b-1}{b+1}\Delta V_{J_{oc_1}} - \frac{b-1}{b+1} V_{nn^+oc} + V_{nn^+oc} \tag{74}$$

which results in eqn. (68a).

For an n^+–p–p^+ cell (Fig. (4b)), holes flowing under a field as well as by diffusion face a collector junction in the newly added p–p^+ junction at $x = d$ and lead to an increase in J_R. However, for electrons flowing by diffusion the p–p^+ junction acts as a blocking barrier and makes them pile up at $x = d$. This attempts to reduce the dark current density J_d by decreasing the magnitude of the electron concentration gradient dn/dx in the bulk p region near the front p–n junction. Both the reduction in $(dn/dx)|_{x=0}$ and the increase in J_R force the n^+ emitter to inject more electrons and the p^+ emitter to inject the necessary number of holes to maintain space charge neutrality in the bulk p region and to satisfy the no-current condition at open circuit. This results in $\Delta V_{J_{oc_2}}$ and

$$V_{pp^+oc} = \frac{kT}{q} \ln\left(\frac{p_{d_2}}{N_A}\right)$$

respectively as the photovoltages developing at the n^+–p and p–p^+ junctions. For high level conditions in the bulk p region, the increased carrier density at $x = 0$ tries to increase the Dember potential by $\{(b-1)/(b+1)\}\Delta V_{J_{oc_2}}$ and the increased carrier density at $x = d$ tries to decrease the Dember potential by $\{(b-1)/(b+1)\}V_{pp^+oc}$. However, owing to the subtractive nature of the Dember potential for the photovoltage of an n^+–p cell, the net improvement in the open-circuit voltage of an n^+–p–p^+ cell is given by

$$\Delta V_{och_2} = \Delta V_{J_{oc_2}} - \frac{b-1}{b+1}\Delta V_{J_{oc_2}} + \frac{b-1}{b+1}V_{pp^+oc} + V_{pp^+oc} \qquad (75)$$

which results in eqn. (68b).

In contrast with a p^+–n–n^+ cell, however, the increase in carrier density in the bulk region of an n^+–p–p^+ cell is inhibited from occurring at $x = 0$. This is because both the concentration gradient of the photogenerated holes and the field in the bulk p region oppose the hole transport from $x = d$ to $x = 0$. The field in the bulk region also inhibits electron transport from $x = 0$ to $x = d$. However, the concentration gradient of electrons due to their photogeneration as well as to their injection from the n^+ emitter favours electron transport from $x = 0$ to $x = d$. A comparison with the p^+–n–n^+ cell shows that conditions favour

$$\Delta V_{J_{oc_1}} > \Delta V_{J_{oc_2}} \qquad \text{and} \qquad V_{pp^+oc} > V_{nn^+oc}$$

Equations (68a) and (68b) in conjunction with the above discussion about the development of ΔV_{och_1} and ΔV_{och_2} reveal that for high level conditions in the bulk region of a p^+–n–n^+ cell the increase in carrier density in the bulk region at the edge of the front p^+–n junction becomes more vital for maximum improvement in the open-circuit voltage of the cell due to the BSF compared with that for low level conditions. In contrast, for an n^+–p–p^+ cell the increase in carrier density in the bulk p region at the edge of the front n^+–p junction becomes less significant for improvement in the open-circuit voltage of the cell for high level conditions in the bulk p region than it had been for low level conditions. Therefore to realize the maximum improvement due to a BSF for high level conditions in the bulk region of a p/n BSF cell, in practice not only the hole-reflecting property of the L–H back junction but also the electron-blocking ability of the front p^+–n junction should be equally important. However, for an n/p BSF cell the electron-blocking capability of the L–H back junction is of principal importance.

A high electron-blocking capability of a p^+–n junction requires a high injection efficiency (nearly unity) of the p^+ emitter to be maintained. Therefore it can be inferred that, for high level conditions in the bulk region of the cells, phenomena such as enhanced front-surface recombination, higher recombination in the front region and an effective band gap narrowing caused by heavy doping in the front region (which all reduce the injection efficiency of the front emitter) may be more detrimental to a p^+–n–n^+ cell than to an n^+–p–p^+ cell.

Fossum and Burgess' experimental data [3] which show an improvement of about 30 - 40 mV in the open-circuit voltage of 10 Ω cm p^+–n–n^+ BSF silicon solar cells after reduction of the front-surface recombination velocity S_F from about 10^5 cm s^{-1} to less than 10^4 cm s^{-1} support the requirement of a high electron-blocking capability of the p^+–n front junction.

Mandelkorn and Lamneck's data [2] on 100 Ω cm n^+–p–p^+ silicon solar cells 250 μm thick show a high sensitivity of V_{ocbh_2} to the maximum photovoltage-generating ability of the p^+–p junction and thereby to the minority-carrier-blocking ability of the p–p^+ junction.

7. Limitation of analysis

The present analysis is based on the concept of effective minority carrier recombination velocity at the rear end of the bulk region of BSF cells. This is valid if $(\mathrm{d}p/\mathrm{d}x)|_{x=d}$ $(\approx(\mathrm{d}n/\mathrm{d}x)|_{x=d}) \leqslant 0$, a basic prerequisite for the validity of eqn. (22) and other equations containing ϵ. For $(\mathrm{d}p/\mathrm{d}x)|_{x=d} \leqslant 0$, ϵ can have a value between 0 and ∞. In the absence of majority carrier injection from the n^+ (or p^+) back region of p^+–n–n^+ (or n^+–p–p^+) cells, a high recombination of minority carriers in the n^+ (or p^+) back region and the influence of the ohmic contact at the back leads to $(\mathrm{d}p/\mathrm{d}x)|_{x=d} \leqslant 0$. As a result, the present analysis is always applicable to low level conditions in the bulk region of p^+–n–n^+ and n^+–p–p^+ cells.

We discussed earlier the fact that for high level conditions the minority carrier blocking due to the BSF coupled with the requirement of quasi-neutrality in the bulk region at open circuit necessitates majority carrier injection by the n^+ (p^+) back region into the bulk n (p) region of a p^+–n–n^+ (n^+–p–p^+) cell. Should the majority carrier injection dominate the minority carrier recombination at $x = d$, $(\mathrm{d}p/\mathrm{d}x)|_{x=d}$ may become positive. For high level conditions such a situation is known to occur for double injection in p^+–n–n^+ or n^+–p–p^+ structures under dark forward bias conditions [19, 29, 30]. However, there is a basic difference: for the dark condition, majority carrier injection is the primary cause of the increase in carrier density at $x = d$ whereas, for an illuminated BSF cell under open circuit, minority carrier blocking is the primary cause of the increase in carrier density at $x = d$.

Earlier discussion showed that, for high level conditions at open circuit, both p^+–n–n^+ and n^+–p–p^+ cells attempt to have a higher carrier density at the p^+ end of their bulk region and thereby attempt to generate an additive photovoltage due to the Dember potential in the bulk region. Thus $(\mathrm{d}p/\mathrm{d}x)|_{x=d} \geqslant 0$ may occur in a front-illuminated n^+–p–p^+ cell whereas it would be much less likely to occur in a front-illuminated p^+–n–n^+ cell. In practice, therefore, it may be achievable in an n^+–p–p^+ cell only if the p^+ back region is thick and is sufficiently heavily doped, and the p–p^+ junction has a high electron-blocking ability.

In general, the present analysis may be applied to front-illuminated p^+–n–n^+ and n^+–p–p^+ silicon solar cells, in practice, if both front and back junctions are shallow in each case. For such a case, a p^+–n–n^+ cell can be expected to show a higher V_{oc} than an otherwise identical n^+–p–p^+ cell if both the cells operate under high level conditions.

The present analysis indicates that a knowledge of the carrier distribution in the bulk region of p^+–n–n^+ and n^+–p–p^+ silicon solar cells based on perfect minority carrier blocking by the L–H junction at open circuit should be able to show why in practice the open-circuit voltages of the two BSF cells are nearly equal under high level conditions.

8. Conclusions

The following conclusions can be drawn.

(1) A BSF improves the open-circuit voltages of p^+–n–n^+ and n^+–p–p^+ cells. The improvement in V_{oc} can be due both to the back reflection of minority carriers from the L–H junction end of the bulk region to the p–n front-junction end of the bulk region and to the blocking of minority carriers by the L–H junction from the bulk region to the heavily doped n^+ or p^+ region on the back side.

(2) For low level conditions in the bulk region, ΔV_{oc} is mainly due to the back reflection of minority carriers and the contribution of the minority carrier blocking is insignificant. For high level conditions, however, the contribution of the minority carrier blocking may also be substantial.

(3) The contribution of the back reflection of minority carriers to ΔV_{oc} is dependent on d/L and the minority carrier recombination velocity at the L–H junction through the parameter ϵ. However, the contribution is independent of the intensity of illumination and ρ_B. The contribution of minority carrier blocking is dependent on d/L and ϵ, and also on the product $J_{sc}L\rho_B$; it increases as the intensity of illumination, L or ρ_B increases.

(4) For low level conditions, the ΔV_{oc} values for p^+–n–n^+ and n^+–p–p^+ cells are equal if d/L and ϵ are the same for both the cells. However, for high level conditions, the ΔV_{oc} values for both the cells are seldom equal.

(5) For high level conditions the open-circuit voltage of a p^+–n–n^+ cell is affected more by decreasing the electron-blocking capability of its p–n (p^+–n) front junction than is the open-circuit voltage of an otherwise identical n^+–p–p^+ cell for a similar reduction in the hole-blocking capability of the p–n (n^+–p) front junction of the n^+–p–p^+ cell.

Thus the minimization of carrier recombination in the exposed front surface and the front region by reducing the front-surface recombination velocity of the minority carriers in the front region and the minimization of the effective band gap narrowing in the front heavily doped region by creating an aiding electric field in the front region are more important for a higher open-circuit voltage of a p^+–n–n^+ silicon solar cell than they are for a higher open-circuit voltage of an n^+–p–p^+ silicon solar cell, when both the cells have high level conditions in their bulk regions.

(6) The minimization of the carrier recombination losses in the heavily doped back regions of n^+–p–p^+ and p^+–n–n^+ silicon solar cells is much more desirable for an n^+–p–p^+ cell than it is for a p^+–n–n^+ cell when both the cells have high level injection conditions in their bulk regions. A deeper L–H junction would therefore be more useful for an n^+–p–p^+ cell than for a p^+–n–n^+ cell.

(7) For high level conditions in the bulk region of a p/n or an n/p BSF cell, the open-circuit voltage is independent of the bulk resistivity of the cell. However, for low level conditions a higher bulk resistivity cell has a lower open-circuit voltage. In contrast, ΔV_{oc} is independent of ρ_B for low level conditions and is higher for a higher ρ_B for high level conditions.

Acknowledgment

The authors wish to thank the Director, National Physical Laboratory, New Delhi, for his permission to publish this paper.

Nomenclature

BSF cell	p^+–n–n^+ or n^+–p–p^+ cell
c	velocity of light
conventional cell	p^+–n or n^+–p cell
d	thickness of the bulk region
d_p	thickness of the shallow front p^+ region of p^+–n–n^+ cell
d_s	thickness of the space charge at the p–n front junction
D_p, D_n	hole and electron diffusion coefficients
E_g	band gap of a semiconductor
h	Planck's constant
J_p, J_n, J	hole, electron and total current densities
J_{sc}	short-circuit current density
J_{scb_1}, J_{scc_1}	J_{sc} of p^+–n–n^+ cell and p^+–n cell
k	Boltzmann constant
L	diffusion length of minority carriers in the bulk n (or p) region
L–H junction	n–n^+ or p–p^+ junction
L_λ	absorption length of photons of wavelength λ in silicon
n	electron concentration at any point x in the bulk region
n_0	electron concentration at $x = 0$ in the bulk region
n_{0b_2}, n_{0c_2}	n_0 for n^+–p–p^+ cell and n^+–p cell for open-circuit condition
n_d	electron concentration at $x = d$ in the bulk region
n_{d_1}	n_d for p^+–n–n^+ cell for open-circuit condition
n_{d_2}	n_d for n^+–p–p^+ cell for open-circuit condition
n_i	intrinsic carrier concentration
n_p	equilibrium electron concentration in the p-type bulk region
n_{ph}	number of photons of wavelength λ falling per unit area per second on the front surface of the cell
n/p BSF cell	n^+–p–p^+ cell
n/p cell	n on p cell (BSF or conventional)
n/p conventional cell	n^+–p cell
N_A	concentration of ionized acceptors in the bulk p region of n/p cells

N_D	concentration of ionized donors in the bulk n region of p/n cells
p	hole concentration at any point x in the bulk region
p_0	hole concentration at $x = 0$ in the bulk region
p_{0b_1}, p_{0c_1}	p_0 for p^+–n–n^+ cell and p^+–n cell for open-circuit condition
p_d	hole concentration at $x = d$ in the bulk region
p_{d_1}	p_d for p^+–n–n^+ cell for open-circuit condition
p_{d_2}	p_d for n^+–p–p^+ cell for open-circuit condition
p_n	equilibrium hole concentration in the n-type bulk region
p/n BSF cell	p^+–n–n^+ cell
p/n cell	p on n cell (BSF or conventional)
p/n conventional cell	p^+–n cell
p–n junction	p^+–n or n^+–p junction
q	electronic charge
R_λ	reflectivity of the front surface of cell for λ
S	effective recombination velocity of minority carriers at the back of the bulk region of p/n or n/p BSF cells
S_F	recombination velocity of minority carriers at the front surface
T	temperature of the device
V_J	photovoltage developed at the p–n front junction
V_{Joc}	V_J at open circuit
V_{Jocb_1}, V_{Jocc_1}	V_{Joc} for p^+–n–n^+ cell and p^+–n cell
V_{oc}	open-circuit voltage
V_{ocb_1}, V_{occ_1}	V_{oc} of p^+–n–n^+ cell and p^+–n cell
V_{ocb_2}, V_{occ_2}	V_{oc} of n^+–p–p^+ cell and n^+–p cell
V_{ocbh_1}, V_{ocbh_2}	V_{oc} of p^+–n–n^+ cell and n^+–p–p^+ cell for high level conditions
V_{ocbl_1}, V_{ocbl_2}	V_{oc} of p^+–n–n^+ cell and n^+–p–p^+ cell for low level conditions
V_{occh_1}, V_{occh_2}	V_{oc} of p^+–n cell and n^+–p cell for high level conditions
V_{occl_1}, V_{occl_2}	V_{oc} of p^+–n cell and n^+–p cell for low level conditions
w	total cell thickness
α_λ	absorption coefficient of silicon for photons of wavelength λ
λ	wavelength of the radiation
λ_g	cut-off wavelength for silicon
μ_p, μ_n	hole and electron mobilities
ΔJ_{sc}	improvement in J_{sc} due to BSF
ΔV_{oc}	improvement in V_{oc} due to BSF
ΔV_{oc_1}, ΔV_{oc_2}	improvement in V_{oc} of p/n cell and n/p cell due to BSF
ΔV_{ocl}, ΔV_{och}	ΔV_{oc} for low level conditions and high level conditions
ΔV_{ocl_1}, ΔV_{ocl_2}	ΔV_{oc} for low level conditions for p/n cell and n/p cell

References

1 J. Mandelkorn, J. H. Lamneck and L. R. Scudder, *Proc. 10th Photovoltaic Specialists' Conf., Palo Alto, CA, November 1973*, IEEE, New York, 1973, p. 207.

2 J. Mandelkorn and J. H. Lamneck, *Proc. 11th Photovoltaic Specialists' Conf., Phoenix, AZ, May 1975*, IEEE, New York, 1975, p. 36.

3 J. G. Fossum and E. L. Burgess, *Appl. Phys. Lett.*, *33* (3) (1978) 238.

4 G. C. Jain, S. N. Singh, R. K. Kotnala and N. K. Arora, Fabrication of p^+–n–n^+ silicon solar cells by simultaneous diffusion of boron and phosphorus into silicon through silicon dioxide, *J. Appl. Phys.*, *52* (7) (1981) 4821.

5 J. Mandelkorn and J. H. Lamneck, *Proc. 9th Photovoltaic Specialists' Conf., Silver Springs, MD, May 1972*, IEEE, New York, 1972, p. 66.

6 M. Wolf, Research for the improvement of silicon solar cell efficiency, *NASA Contract Rep.*, January 1971 (NASA Grant NGL 39-010-001).

7 J. Michel, A. Mircea and E. Fabre, *J. Appl. Phys.*, *46* (1975) 5043.
8 M. P. Godlewski, C. R. Baraona and H. W. Brandhorst, Jr., *Proc. 10th Photovoltaic Specialists' Conf., Palo Alto, CA, November 1973*, IEEE, New York, 1973.
9 J. H. Brattain and C. G. B. Garett, *Ann. N.Y. Acad. Sci.*, *58* (1954) 951.
10 J. Mandelkorn and J. H. Lamneck, *J. Appl. Phys.*, *44* (1973) 4885.
11 J. G. Fossum, *IEEE Trans. Electron Devices*, *24* (1977) 332.
12 O. von Roos, *J. Appl. Phys.*, *49* (1978) 3503.
13 O. von Roos, *J. Appl. Phys.*, *50* (1979) 5371.
14 J. R. Mallinson and P. T. Landsberg, *Proc. R. Soc. London, Ser. A*, *355* (1977) 115.
15 J. G. Fossum, E. L. Burgess and F. A. Lindholm, *Solid-State Electron.*, *21* (1978) 729.
16 Chung-Yuan Wu and Wen-Zen Shen, *Solid-State Electron.*, *23* (1980) 209.
17 M. Wolf, *Energy Convers.*, *11* (1971) 63.
18 G. C. Jain, A. Prasad and S. N. Singh, *Solid-State Electron.*, *17* (1974) 431.
19 S. N. Singh, Study of high injection phenomenon in junction diodes, *Ph.D. Thesis*, Agra University, 1975.
20 S. M. Sze, *Physics of Semiconductor Devices*, Wiley, New York, 1969.
21 W. Shockley and W. T. Read, *Phys. Rev.*, *87* (1952) 835.
22 J. Lindmayer and J. F. Allison, The violet cell. An improved silicon solar cell, *COSMAT Tech. Rev.*, *3* (1) (1973) 1 - 22.
23 J. R. Hauser and P. M. Dunbar, *IEEE Trans. Electron Devices*, *24* (1977) 305.
24 B. Ellis and T. S. Moss, *Solid-State Electron.*, *13* (1970) 1.
25 G. C. Jain and W. B. Berry, *Transport Properties and Solid State Energy Conversion*, Tata McGraw-Hill, New Delhi, 1972.
26 H. Dember, *Phys. Z.*, *32* (1931) 554 and 856; *33* (1932) 209.
27 J. G. Fossum and F. A. Lindholm, *IEEE Trans. Electron Devices*, *24* (1977) 325.
28 N. G. Tarr, D. L. Pulfrey and P. A. Iles, *Appl. Phys. Lett.*, *35* (3) (1979) 258.
29 N. R. Howard and G. W. Johnson, *Solid-State Electron.*, *8* (1965) 275.
30 R. W. Knepper and A. G. Jordon, *Solid-State Electron.*, *15* (1972) 45.